

Theoretical Investigations of Ti-Based Binary Shape Memory Alloys

Rita John¹, Hannah Ruben^{2,3}

¹Department of Theoretical Physics, University of Madras, Chennai, India; ²Post Graduate Department of Physics, Women's Christian College, Chennai, India; ³Mother Teresa Women's University, Kodaikanal, India.
Email: rita_john@sify.com, hancath2007@yahoo.co.in

Received June 15th, 2011; revised July 8th, 2011; accepted August 17th, 2011.

ABSTRACT

The electronic structure and ground state properties of TiX (X = Fe, Ni, Pd, Pt and Cu) type Shape Memory alloys have been calculated using the self consistent Tight-Binding Linear Muffin Tin Orbital (TB-LMTO) method. The systematic total energy studies made on TiX alloys in both B2 and (B19/B19') structures successfully explain the structural stability of these compounds. The equilibrium lattice parameters, bulk moduli (B_0), cohesive energy (E_{coh}) and heat of formation (ΔH) are calculated for these systems and compared with the available experimental and other theoretical results. The bonding nature of these TiX alloys is analyzed via the density of states (DOS) histogram.

Keywords: Shape Memory Alloys, TB-LMTO, B2-B19 Phases, Structural Parameters

1. Introduction

Martensitic alloys have been a hot topic for several decades due to shape memory effect and many other peculiar properties present during their martensitic phase transformation [1,2]. A lot of experimental and theoretical works have been devoted to study this phenomenon yet many aspects of the transformation are still elusive. It has stimulated many investigations in exploring the difference in electronic structure of different structural phases involved in the transformation from martensite phase (B19/B19') to austenite phase (B2).

To investigate Martensitic phase transformation from the electronic point of view, Ye *et al.* [3] have used first principles total energy calculations to show some interesting correlations between the relative stability of B2 and (B19/B19') phases with the electronic structure for TiNi, TiPd and TiPt alloys.

The main objective of the paper is to study the electronic and structural properties of TiX (X = Fe, Ni, Pd, Pt and Cu) alloys in both (B2) and (B19/B19') phases calculated using the self consistent Tight-Binding Linear Muffin Tin Orbital (TB-LMTO) method. The paper is divided into six sections. Section 2 gives a brief outline of the computational details of the Tight-Binding Linear Muffin Tin Orbital scheme. The results of the total energy calculations obtained for cubic (B2) and orthorhombic/monoclinic (B19/B19') phases of TiX alloys are

presented in Section 3. The band structure and density of states (DOS) for TiX (X = Fe, Ni, Pd, Pt and Cu) alloys in both phases are reported in Section 4. Section 5 deals with the theoretically calculated cohesive energy, heat of formation which are compared with the experimentally reported available values. The bulk modulus values obtained for the alloys using the universal equation of state (UEOS) analysis are reported in Section 6. The important conclusions arrived from the above studies are given in the last Section.

2. Method of Calculation

The band structure and total energy studies are made within the atomic-sphere approximation by means of Tight Binding-Linear Muffin Tin Orbital method (TB-LMTO) [4], which is the exact transformation of Andersen's linear muffin-tin orbitals [5] to localize short-ranged or tight-binding orbitals. The potential is calculated within the density-functional prescription under local-density approximation (LDA) using the parameterization scheme of von Barth and Hedin [6]. The TB (screened) representation of the LMTO method makes the computation fast for the following reasons: 1) the MTO's are linear in energy and hence, unlike the augmented plane-wave or Korringa-Kohn-Rostoker methods we can get the eigen values within single diagonalization; 2) a solution to an eigen value equation of size only 9×9

(for s, p, d electron elements) per atom at each point in reciprocal space is required; 3) The screened structure constant for each atom needs only up to second-nearest-neighbor atoms. In the band structure calculations, the valence electronic configurations for TiFe, TiNi, TiPd, TiPt and TiCu are as Ti: $3d^2 4s^2$, Ni: $3d^8 4s^2$, Pd: $4d^{10}$, Pt: $5d^9 6s^1$ and Cu: $3d^{10} 4s^1$ respectively. They are chosen to represent the basis set for our calculations. The d electrons are treated as valence electrons unlike earlier pseudopotential based calculations. In our calculations, the s, p, d partial waves have been used (*i.e.*, maximum angular momentum $l_{\max} = 2$). Apart from this, the combined correction terms are also included, which account for the non-spherical shape of the atomic cells and the truncation of higher partial waves ($l > 2$) inside the sphere so as to minimize the errors in the LMTO method. To exclude additional freedom in the choice of computational parameters the same Weigner-Seitz (WS) radius is chosen for all atoms and the calculated overlaps between the various atomic spheres in this WS radius are within the allowed range of the atomic-sphere approximation. The atomic position coordinates used for B2 and B19 structures are (0, 0, 0), (0.5, 0.5, 0.5) and (0, 0, 0) and (0.5, 0.0, 0.5) all alloys respectively.

The tetrahedron method for the Brillouin zone (*i.e.*, k space) integration has been used with its latest version, which avoids misweighing and corrects error due to the linear approximation of the bands inside each tetrahedron [7].

3. Total Energy Calculations

In order to determine the phase stability of both B2 and

(B19/B19') crystal structures in **Figure 1**, we have calculated the total energy for each alloy with different lattice constants in the reduced and extended experimental volumes for all the compounds. The self consistent iterations were carried out with an accuracy of 10^{-4} Ryd for eigen values, using 96 k points in the irreducible wedge of the first Brillouin zone (IBZ) of orthorhombic/monoclinic structures and 72 k points in the IBZ of cubic structures.

The total energy curves for TiX (X = Fe, Ni, Pd, Pt and Cu) alloys in B2 and (B19/B19') structures for different reduced and extended volumes are shown in **Figure 2**. The equilibrium lattice constants of the above mentioned systems in both phases are calculated. From **Table 1**, the theoretically obtained equilibrium lattice constants are underestimated compared to the experimental values [8],

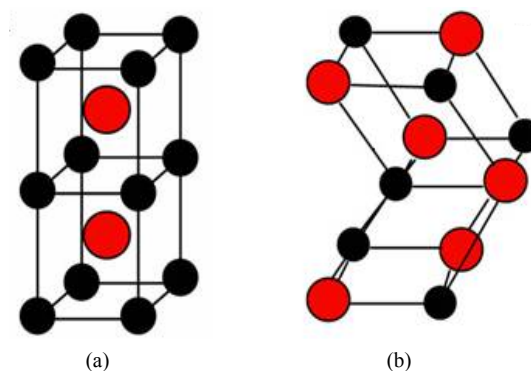


Figure 1. (a) Austenite (B2) lattice structure and (b) martensite (B19/B19') lattice structure.

Table 1. Experimental and Theoretical lattice constants (a, b, c) in Å of Ti X (X = Fe, Ni, Pd, Pt, Cu) alloys.

Alloy	Type	Present work			Theoretical			Experimental		
		a	b	c	a	b	c	a	b	c
TiFe	B2	2.9156			2.987 ^[a]			2.976 ^[a]		
	B19	2.7581	4.4204	3.934						
TiNi	B2	2.9714			3.023 ^[a]			3.015 ^[a]		
	B19	2.512	4.028	3.582	2.859 ^[b]	4.582 ^[b]	4.078 ^[b]			
	B19'	2.8801	4.5792	4.0321	2.898 ^[c]	4.108 ^[c]	4.646 ^[c]			
TiPd	B2	3.1263			3.191 ^[a]			3.18 ^[a]		
	B19	2.7030	4.6010	4.3780	2.79 ^[b]	4.81 ^[b]	4.52 ^[b]	2.81	4.89	4.52
TiPt	B2	3.1374			3.205 ^[a]			3.192 ^[a]		
	B19	2.6464	4.5476	4.2843	2.81 ^[b]	4.83 ^[b]	4.55 ^[b]	2.76 ^[a]	4.84	4.59
TiCu	B2	3.0275			3.07 ^[a]					
	B19	2.8966	4.6427	4.1320						

^[a]Reference [9]; ^[b]Reference [10]; ^[c]Reference [11].

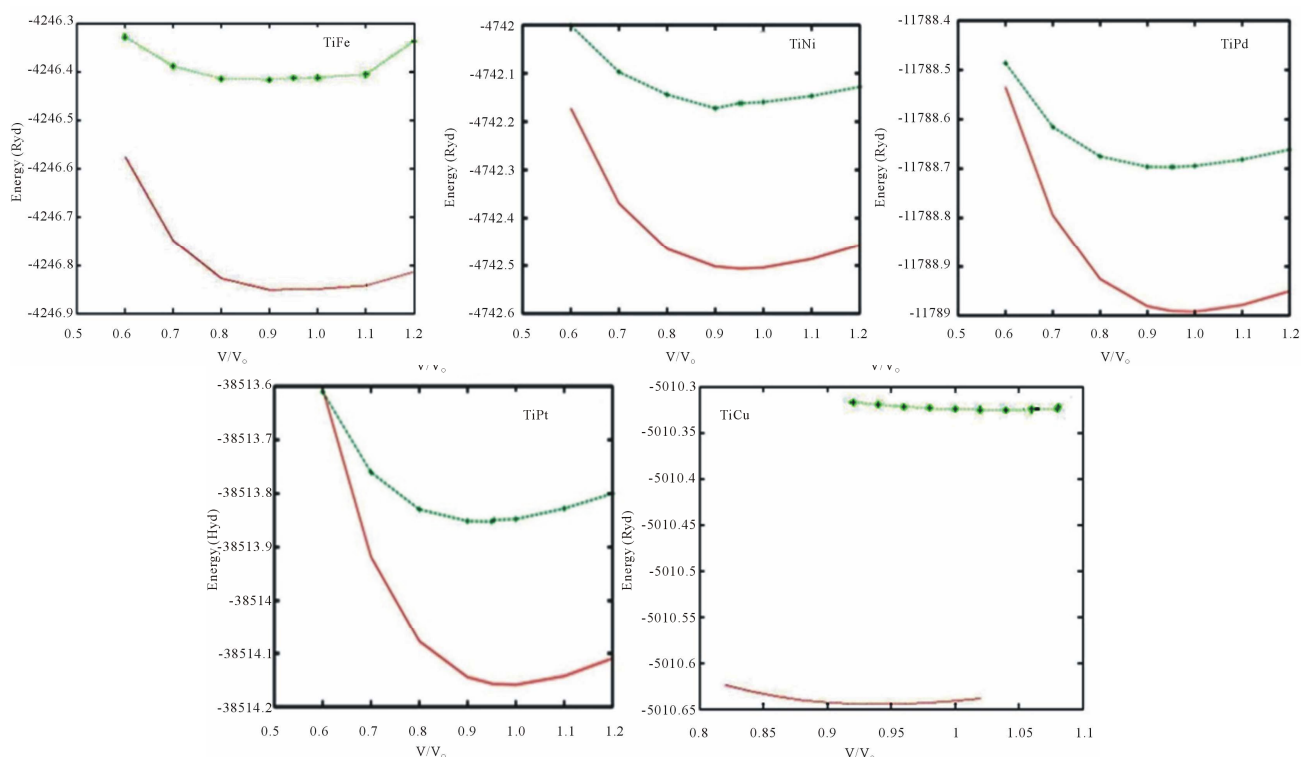


Figure 2. Total energy as a function of volume for TiX (X = Fe, Ni, Pd, Pt and Cu) alloys. Continuous line indicates B2 structure and line with points indicates B19'/B19 structure.

and this is partly ascribed to the local density approximation (LDA) used in the calculations. To minimize the deviations, it is argued that the zero point vibrations have to be included in the calculation [12].

The total energy curves of TiX (X = Fe, Ni, Pd, Pt and Cu) alloys in B2 and (B19/B19') phases, as seen in **Figure 2** show that these alloys are stable in B2 structure [13] though the energy difference between the two is very small of the order of 0.2502 Ry/F.u.

4. Band Structure and Density of State Studies on TiX (X = Fe, Ni, Pd, Pt and Cu) Alloys

The correlation of structural stability with electronic structure is performed using band structure calculations [14]. The band structures of TiX (X = Fe, Ni, Pd, Pt and Cu) alloys have the same generic nature in B2 and B19 structures respectively. They are plotted along high symmetry lines; **Figures 3(a)** and **3(b)** show the band structures of TiX alloys in both phases for several symmetry directions in k-space. The (B19/B19') structure of TiX alloys possesses lower symmetry leading to splitting of degenerate bands in the interior of Brillouin zone as seen in **Figure 3(b)**. The size of the Brillouin zone is twice as big as B2 structure since it possesses four atoms per unit cell. Hence the band structure of (B19/B19') phase has

complicated Brillouin zone compared to B2.

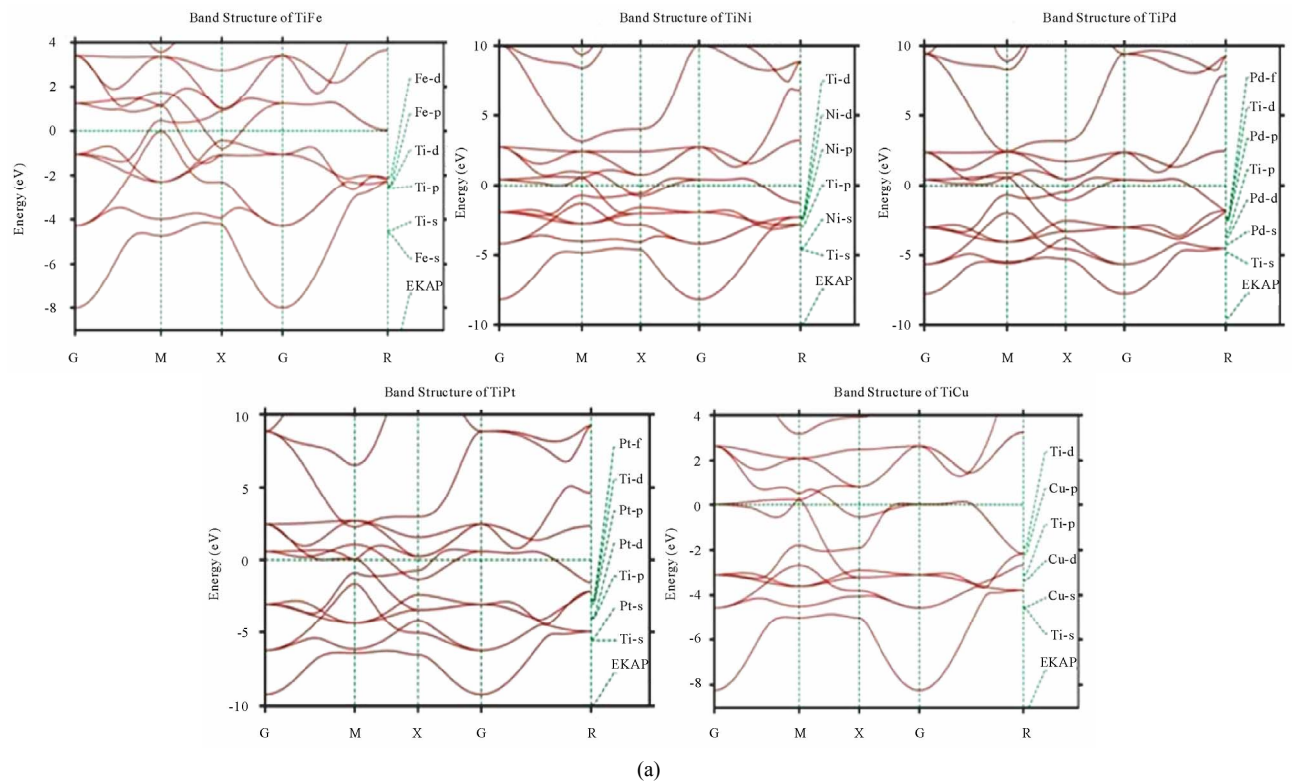
The band structure of TiNi in B2 structure is shown in **Figure 3(a)**. The s-orbitals of Ti and Ni sites around -8 eV are the lowest lying valence bands and do not contribute much in deciding the properties of these alloys. The top most valence band below E_F between -4 eV and -2 eV are due to Ti-d states followed by Ni-d states. Below them, the contribution from Ni-p state predominates.

The band dispersions of (B19/B19') phase have similar generic nature as B2 at more bound states as seen in **Figure 3(b)**, yet there are significant differences that can be detected at higher energies near the Fermi level E_F .

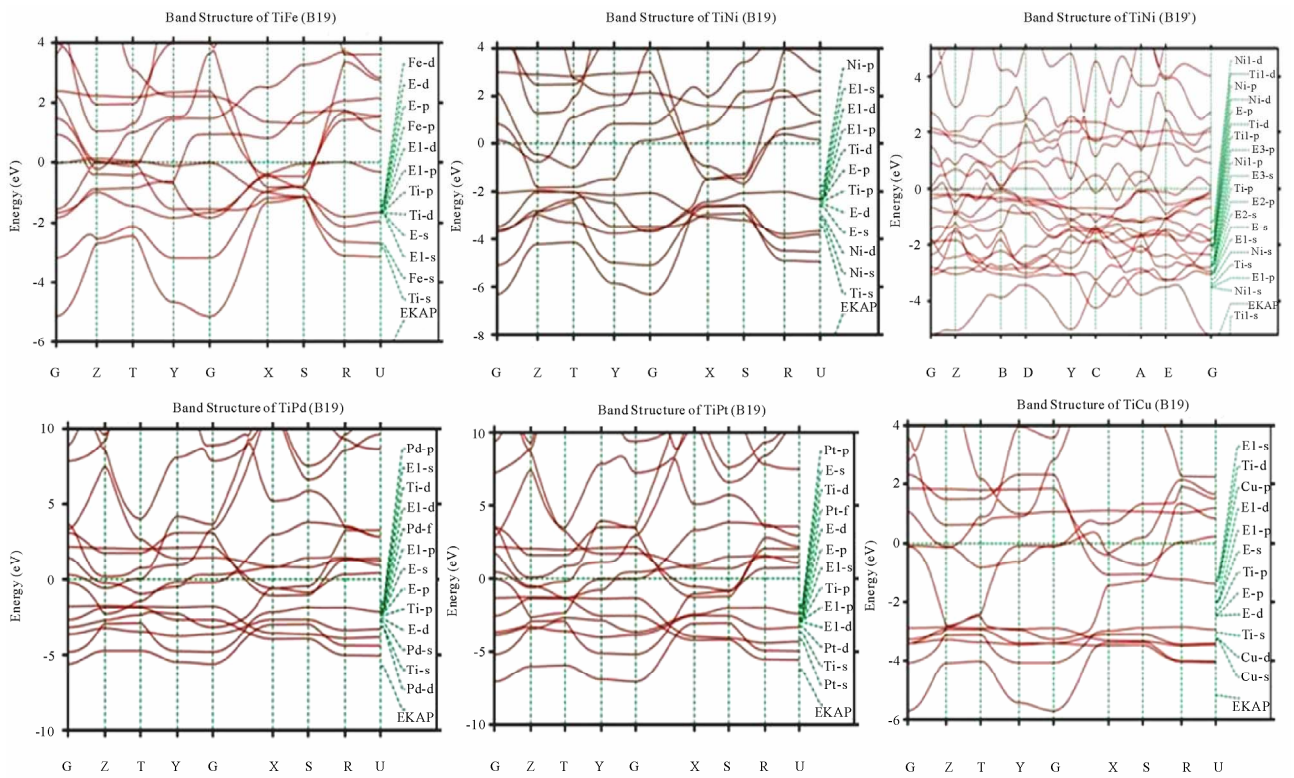
This is reflected in the corresponding density of states (DOS) curve there by influencing various physical properties such as susceptibilities and optical conductivities in both phases [15].

The widths of the valence band for all alloys are tabulated in **Table 3**. We observe the width of the band to be narrower for (B19/B19') phase compared to B2. Hence the interactions between Ti and X (X = Fe, Ni, Pd, Pt and Cu) atoms are much stronger in (B19/B19') phase compared to B2, which is also reflected in their corresponding DOS curves [15].

In both phases TiPt possess wider bandwidth compared to all other TiX (X = Fe, Ni, Pd and Cu) alloys. The higher localization of Pt atom towards the bound



(a)



(b)

Figure 3. (a) Band structure of TiX (X = Fe, Ni, Pd, Pt and Cu) in B2 phase at $V/V_0 = 1$; (b) Band structure of TiX (X = Fe, Ni, Pd, Pt and Cu) in B19 phase at $V/V_0 = 1$.

state in comparison to other X (X = Fe, Ni, Pd, and Cu) atoms results in decrease in overlap of bands between Ti and Pt. This weakens the interaction between the two, and consequently the strength of the covalent bonding between them is decreased.

Density of States

To study the phase stability at microscopic level, the DOS are calculated for the TiX (X = Fe, Ni, Pd, and Cu) alloys at their equilibrium volumes and are plotted using linear tetrahedron method. In present study, the double peak structure is the most typical two peak structure of the total DOS curve which is shown in **Figures 4(a)** and **4(b)**.

The DOS curves for B19/B19' structures are similar in nature to that of the B2. Due to lower symmetry the DOS peaks of the B19 and B19' structures tend to be broader than B2. There are some changes noticed in the lower portion of the DOS curves of B19/B19' structure at a range of ± 1.5 eV around Fermi. From **Figures 4(a)** and **4(b)** we observe the dividing dip of the DOS in B2 structure at about -1.5 eV around Fermi becomes less conspicuous in B19 structures. In B19' structure, near the Fermi level within a range of ± 1.5 eV there is an upward shift of the dip of the DOS curve.

The DOS curve of TiFe alloy in both phases is found to be in good agreement with the reported results of Y. Ye *et al.* The typical feature of the total DOS curve of TiFe in B2 phase is the presence of pseudo gap. Two mechanisms were proposed for the formation of pseudo gap in the binary alloys [16]. One is of ionic origin, and other is owing to hybridization effects. As the electro negativity difference between Ti and X is low, the ionicity does not play a major role on bonding behavior of these compounds. Consequently the pseudo gap present in TiFe alloys is believed to be due to covalent hybridization between Ti and Fe atoms. Such a strong hybridization gives not only an important mixing between the states of conduction bands but also leads to a separation of bonding states creating a pseudo gap.

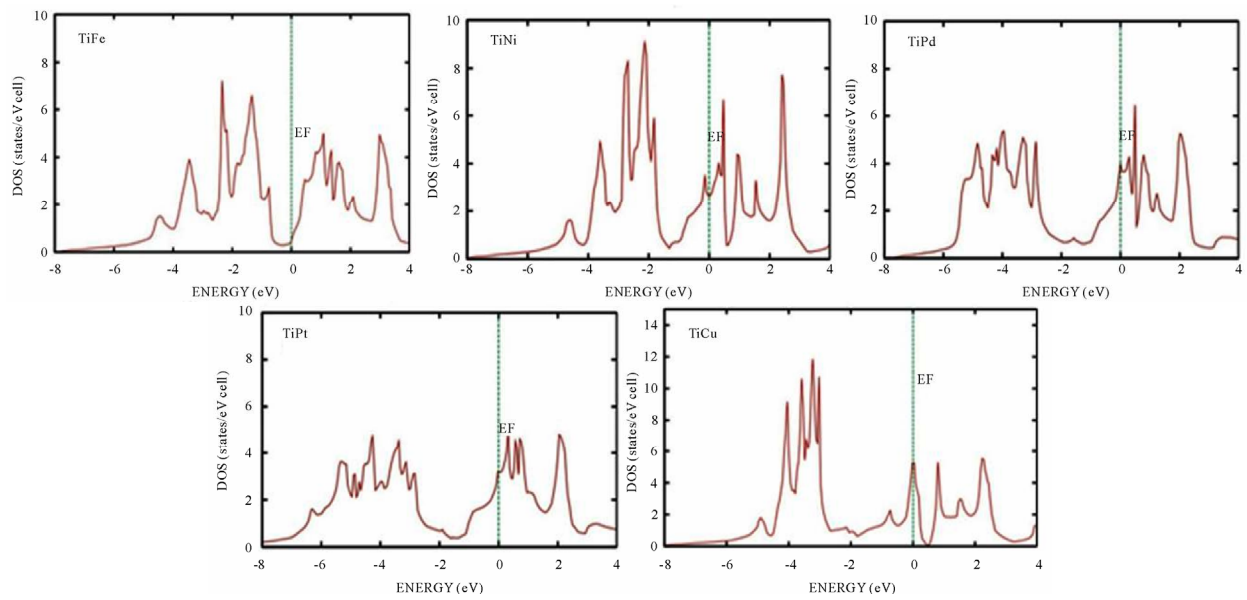
In the present work we observe that in B2 structure the shape of the DOS curve of TiNi is similar to TiFe. For both alloys the E_F falls on a dip as shown in **Figure 4(a)**. It is well known fact that if the Fermi level E_F falls on the dip, the corresponding structure may be regarded as a save energy system as compared with one whose Fermi level E_F does not fall on a dip. Therefore TiFe and TiNi alloys are more stable than other transition metals Pd, Pt and noble metal Cu. On going from TiPd, TiPt and TiCu the B2 structure becomes relatively less stable, as the Fermi level E_F shifts from the dip towards higher peaks of the DOS [17]. This is accounted by the increase in valence electrons which will tend to shift the Fermi level

E_F from the dip towards the anti-bonding states. From **Figure 4(b)** similar dip is observed for TiPd, wherein the Fermi level E_F falls on the dip. Hence TiNi and TiFe in B2 structure and TiFe and TiPd in B19 structure have low $N(E_F)$ values at Fermi and are considered to be most stable structures. However the stability of TiPd in B19 contradicts the inference for the total energy calculations shown in **Figure 2**. As the energy of TiPd at Fermi is lower for B2 (-0.0523 eV) when compared to B19 (0.0271 eV) structure, TiPd can be considered to be stable in B2 structure. This is in line with the results reported by Ravindran *et al.* [17] in the case of Ni_3Al and $Ni_3Al_{0.75}Nb_{0.25}$.

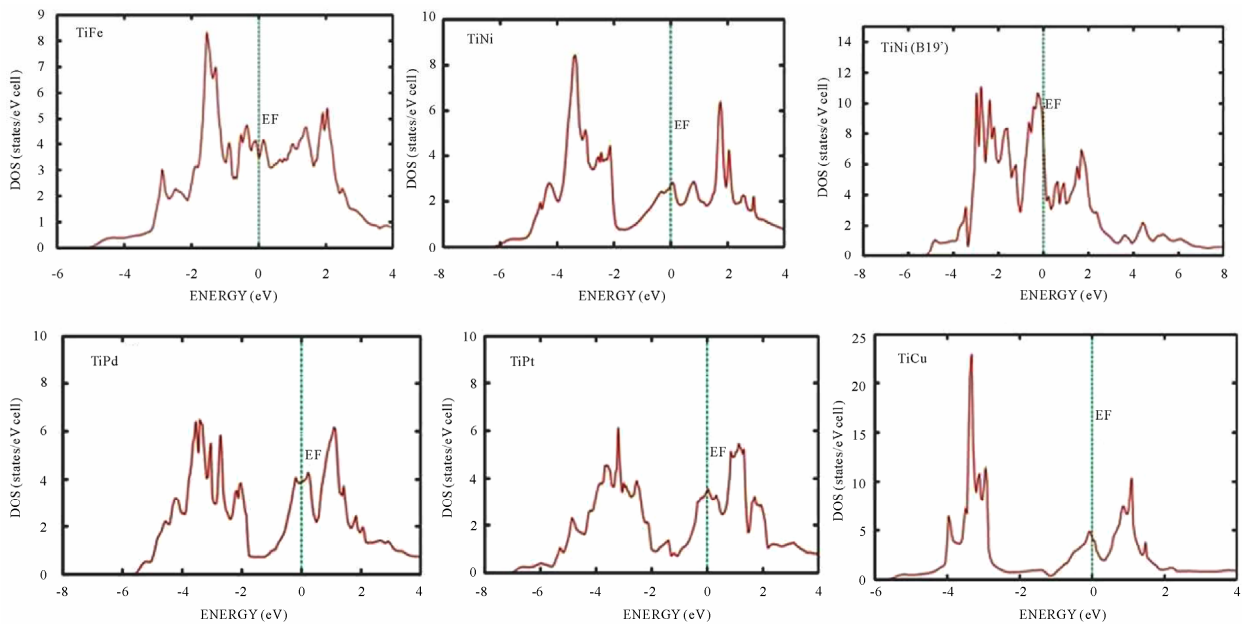
As the electrons around E_F play an important role in deciding the electronic, structural and mechanical properties of the alloys, we carry out the investigations on the electronic structure histogram using the projected DOS of TiX alloys. General nature of the DOS histograms of all TiX (X = Fe, Ni, Pd, Pt and Cu) alloys are observed to be similar of which the DOS histogram of TiNi alloy is shown in **Figure 4(c)**. consists of three parts 1) the peak present in the lower energy part of the DOS curve is mainly due to the localized or tightly bound s-electrons of Ni and Ti atoms; 2) the bonding states of Ti-d and Ni-p orbitals are near (to the left of) the Fermi level E_F ; 3) the DOS curve due to anti-bonding states. It is found that Ti-s state and Ni-s-state electrons in TiX alloy are localized and its effect in bonding is very small. Thus the electrons from Ti-d and Ni-d, Ni-p states predominately contribute to the density of states at the Fermi level E_F .

In order to explore the role of X (X = Fe, Ni, Pd, Pt and Cu) atoms in the Ti-based alloys we compare the d-partial DOS curves of these alloys as shown in **Figures 4(d)** and **4(e)**. We observe that the d-states of Ti atom at Fermi shows a dominance compared to X (X = Ni, Pd, Pt, Cu) atoms. The XPS studies by Shabaloskaya *et al.* [18] show that as elemental X atoms combine with Ti atom to form TiX (X = Ni, Pd, Pt, Cu) compound, it results in enhancement of localization of d-electron of X atoms towards bound state. Hence the intensity of the d-band of X atom in TiX (X = Ni, Pd, Pt, Cu) alloys considerably decreases at Fermi and that of Ti atom increases. However in case of TiFe alloy, we observe the d-states of Fe atom to dominate that of Ti at Fermi. This is because as elemental Fe forms TiFe compound on combination with Ti atom, the position of d-band peaks of Fe atom does not change [19], (*i.e.*) (the Fe atom does not undergo much localization as other X (X = Ni, Pd, Pt, Cu) atoms). Thus the d-band of Fe atom shows much dominance at Fermi when compared to that of d-band of Ti.

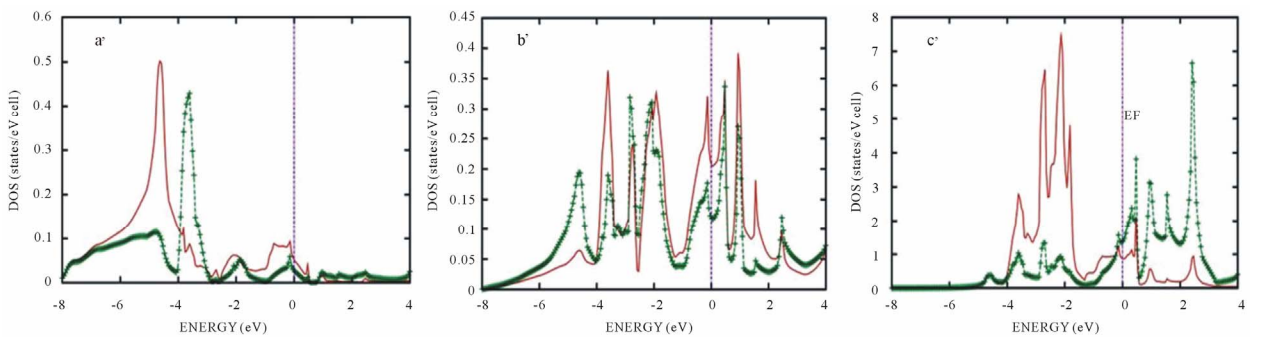
This is also well supported by the DOS values of TiX (X = Ni, Pd, Pt, Cu) alloys at E_F which are tabulated in **Table 2**. From **Table 2** in both B2 and B19 structure, we



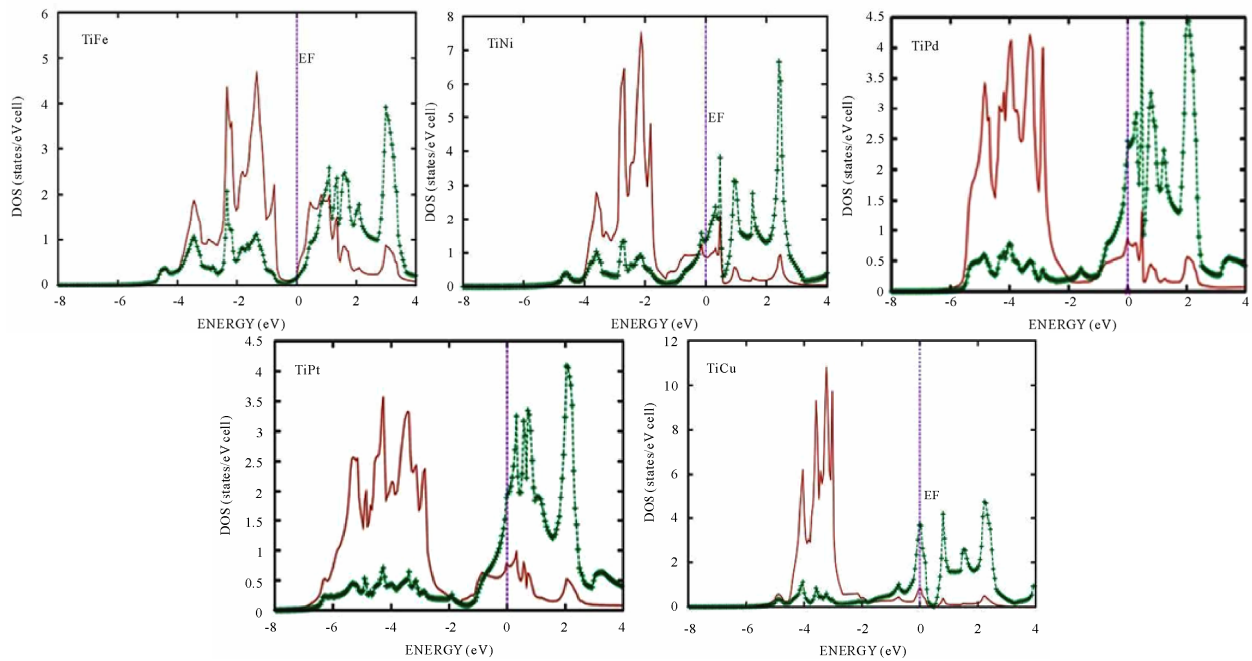
(a)



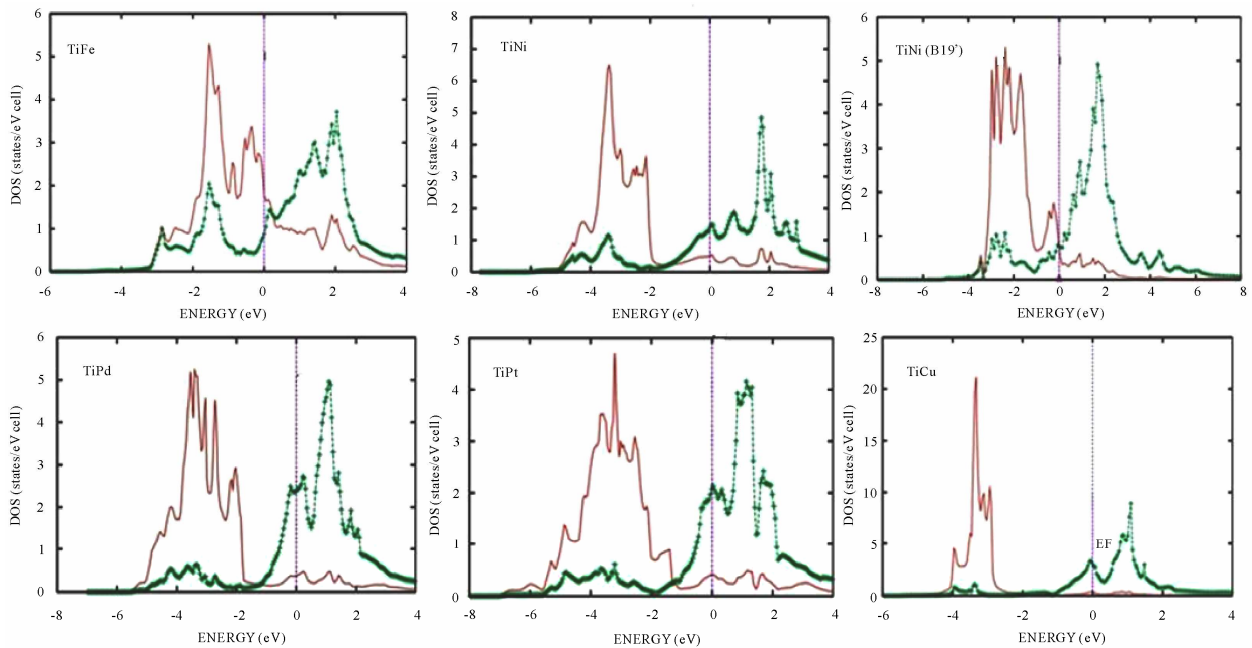
(b)



(c)



(d)



(e)

Figure 4. (a) Total DOS structure of TiX (X = Fe, Ni, Pd, Pt and Cu) in B2 Phase; (b) total DOS structure of TiX (X = Fe, Ni, Pd, Pt and Cu) in B19 Phase; (c) (a') s-Partial DOS (b') p-Partial DOS (c') d-Partial DOS of TiNi in B2 phase. Line with points indicate Ti atom and continuous line indicate Ni atom; (d) d-Partial DOS of TiX (X = Fe, Ni, Pd, Pt and Cu) alloys in B2 phase. Line with points indicate Ti atom and continuous line indicates X atoms; (e) d-Partial DOS of TiX (X = Fe, Ni, Pd, Pt and Cu) alloys in B19 phase. Line with points indicate Ti atom and continuous line indicates X atoms.

observe the d-DOS value of Ti at E_F in general increases from TiFe to TiCu along which the stability of phases decreases. The increase in degeneracy of the d-states of

Ti at Fermi level E_F decreases the phase stability as suggested by Wang *et al.* [20]. Except for Fe atom, the d-DOS contribution of X atom to DOS at Fermi level E_F , is

Table 2. The DOS value at the E_F in TiX (X = Fe, Ni, Pd, Pt and Cu) alloys.

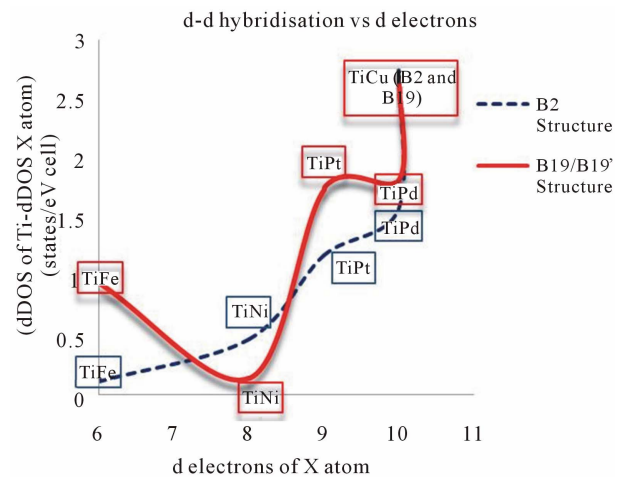
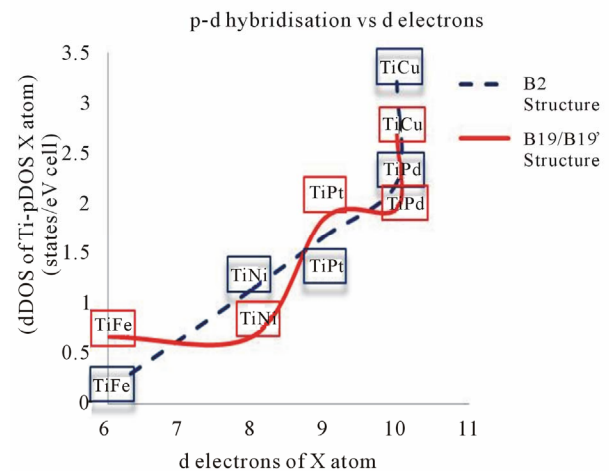
ALLOYS	TiFe		TiNi			TiPd		TiPt		TiCu	
PHASE	B2	B19	B2	B19	B19'	B2	B19	B2	B19	B2	B19
$N_d(E_F)$ of Ti	0.1841	0.8607	1.353	1.9886	0.7651	2.4000	2.1904	1.9230	2.1428	3.5596	2.9885
$N_d(E_F)$ of X	0.2957	1.8116	0.882	0.7272	0.6262	0.8285	0.3714	0.7500	0.4000	0.8217	0.2952
$N_p(E_F)$ of Ti	0.0377	0.1435	0.117	0.1181	0.0198	0.1950	0.1795	0.1034	0.1568	0.3397	0.1551
$N_p(E_F)$ of X	0.0442	0.1982	0.205	0.1948	0.0982	0.1971	0.2431	0.2571	0.2857	0.3586	0.2665
$N_s(E_F)$ of Ti	0.0032	0.0781	0.029	0.0925	0.0188	0.0558	0.1121	0.0465	0.1037	0.0174	0.0958
$N_s(E_F)$ of X	0.0045	0.1040	0.047	0.1318	0.0256	0.0941	0.0636	0.0655	0.0409	0.0174	0.0443
$N_T(E_F)$ of Ti	0.2161	1.1177	1.470	1.9318	0.7810	2.6300	2.4761	2.0769	2.3714	3.9669	3.3383
$N_T(E_F)$ of X	0.3135	2.0951	1.117	1.0455	0.7555	1.2280	0.6984	1.1363	0.7619	1.1467	0.6021
$N_T(E_F)$ of TiX	0.4427	3.4932	2.588	3.4285	3.9149	3.8636	3.6000	3.2000	3.5600	5.0767	4.3034

relatively small when compared to Ti. We observe Ti-d state is virtually twice as high as the corresponding state of X atom, resulting in weakening of $d_{Ti}-d_X$ directional bond between them. The main part of the bonding state of d-electrons of X site gradually move towards the bottom of the valence band while the anti-bonding state of d-electrons at Ti site becomes gradually strong, thereby weakening the $d_{Ti}-d_X$ directional bond between them.

Thus as the atomic number of X (X = Fe, Ni, Pd, Pt, Cu) atom increases, its d-state in both B2 and B19 phases become more localized, the maximum of d-bands shifts towards the bottom of the valence band, and the X contribution to the density of states (DOS) at the Fermi level $N(E_F)$, degrades (Table 2). While the d electron contribution of X to the DOS at E_F decreases, the d electron contribution of Ti increases to such an extent that in TiPd and TiCu, the X contribution to $N(E_F)$ is almost negligible. Hence the d-DOS localization accompanied by a spatial localization of d electrons of X (X = Fe, Ni, Pd, Pt, Cu) atom results in weakening of the d-d covalent bonds between the alloy components thus, destabilizing the phase. Similarly from Table 2 we observe the p contribution of X atom to DOS at E_F are relatively smaller than d contribution of X. Hence the p-d hybridisation will be less pronounced for all these alloys.

In order to compare the nature of hybridisation in each alloy we have plotted graphs between the difference in d DOS of Ti and X with d electrons of X atoms, and difference in d DOS of Ti and p of X atom with d electron of X atoms as shown in Figures 5 and 6. In comparing Figures 5 and 6 we observe that both hybridisations follow the similar trend. The d-d and p-d hybridisations are well pronounced for TiFe in B2 and B19 structure.

In case of TiNi d-d hybridization in B19' structure dominates. For TiPd and TiPt p-d hybridization in B19

**Figure 5. d-d hybridisation of TiX (X = Fe, Ni, Pd, Pt and Cu) in B2 and B19/B19' phase.****Figure 6. p-d hybridisation of TiX (X = Fe, Ni, Pd, Pt and Cu) in B2 and B19/B19' phase.**

structure is much pronounced than d-d hybridization. And both the hybridizations are very less pronounced in TiCu.

5. Cohesive Energy and Heat of Formation

The cohesive energy of a material is a fundamental property which has long been the subject of theoretical and computational approaches. The chemical bonding is a mixture between covalent, ionic, and metallic bonding and therefore the cohesive energy cannot be determined reliably from simple models. Thus, first principles calculations based on density functional theory (DFT) have become a useful tool to determine the cohesive energy of the solids. In this connection, the cohesive energy of TiX (X = Fe, Ni, Pd, Pt and Cu) alloy is calculated by using the expression

$$\text{TiX}_{\text{coh}}^{\text{AB}} = \left[\text{Ti}_{\text{atom}}^{\text{A}} + \text{X}_{\text{atom}}^{\text{B}} \right] - \text{TiX}_{\text{total}}^{\text{AB}} \quad (1)$$

$\text{TiX}_{\text{total}}^{\text{AB}}$ refers to the total energy of the TiX alloy at equilibrium lattice constants and $\text{Ti}_{\text{atom}}^{\text{A}}$ and $\text{X}_{\text{atom}}^{\text{B}}$ are the atomic energies of the pure Ti and X (X = Fe, Ni, Pd, Pt and Cu) constituents calculated semi-relativistically. To determine the heat of formation, we have first calculated the total energy of Ti element and X (X = Fe, Ni, Pd, Pt and Cu) corresponding to their respective equilibrium lattice parameters. The free energy of formation or the heat of formation (ΔH) can be obtained from the following relation:

$$(\Delta H)^{\text{AB}} = \text{TiX}_{\text{total}}^{\text{AB}} - \left[\text{Ti}_{\text{solid}}^{\text{A}} + \text{X}_{\text{solid}}^{\text{B}} \right] \quad (2)$$

where $\text{TiX}_{\text{total}}^{\text{AB}}$ refers to the total energy of TiX (X = Fe,

Ni, Pd, Pt and Cu) alloy at equilibrium lattice constants and $\text{Ti}_{\text{solid}}^{\text{A}}$ and $\text{X}_{\text{solid}}^{\text{B}}$ is the total energy of the pure elemental constituents.

The calculated values of the cohesive energies and heat of formation of all systems are given in **Table 3**. The systematic errors in total energy due to the ASA are cancelled due to the nature of the formula of differences in total energy leading to a reasonably accurate formation of energy.

The cohesive energies of the alloys are slightly lower in (B19/B19') phase compared to B2 phase except for TiNi. This indicates that atoms in B2 phase are strongly bound with better mechanical strength than (B19/B19') phase. In the case of TiNi the cohesive energy is much higher in B19' phase compared to B2 phase indicating that bonding effect is much stronger in B19' phase compared to B2 phase. This is due to strong $d_{\text{Ti}}-d_{\text{X}}$ directional bonding between Ti and Ni atom which can also be seen from **Table 2**. It is observed from **Figure 7** that the cohesive energies of 5d transition series is higher compared to 3d series which is due to higher localization of Pd and Pt atom compared to 3d elements such as Fe, Ni and Cu. This confirms the experimental studies, that 5d elements of larger cohesive energies have higher melting point [21].

From **Table 3**, the study on heat of formation show that the ordering energy values except for TiFe are much higher in (B19/B19') phase compared to B2 phase which is seen in **Figure 8**. This is a positive indication of strong directional bonding leading to brittleness in (B19/B19') phase. The present theoretical values of heat of formation

Table 3. The theoretically calculated cohesive energy (E_{coh} in eV/F.u), heat of formation (ΔH in eV), bulk modulus (B_0 in Mbar) for TiX (X = Fe, Ni, Pd, Pt and Cu) alloys.

Alloy	Type	E_{coh} (eV/F.u)	$-\Delta H$ (eV)	B_0 (Mbar)	e/a	$N(E_F)$ (eV)	Width of the valence band (eV)
TiFe	B2	1.9955	0.3761	3.3084	6	0.4427	7.9577
	B19	1.9953	0.3755	1.6083		3.4931	5.1720
TiNi	B2	2.4187	0.640 0.66 ^[a]	2.2984, 1.56 ^[a]	7	2.5881	8.1818
	B19	2.4186	0.750	1.5891		3.4285	6.2063
	B19'	2.8262	0.9520	1.5603		3.9149	5.0117
TiPd	B2	6.0124	1.033 0.92 ^[a]	2.8446	7	3.8636	7.8409
	B19	6.0122	2.582	3.0112		3.6000	5.777
TiPt	B2	19.6423	1.630 1.49 ^[a]	2.1717	7	3.2000	9.2045
	B19	19.6420	1.879	3.4499		3.5600	7.1379
TiCu	B2	2.6187	2.2448	0.8851	7.5	5.0784	8.2688
	B19	2.6185	2.2444	0.9847		4.3036	5.8078

^aReference [3].

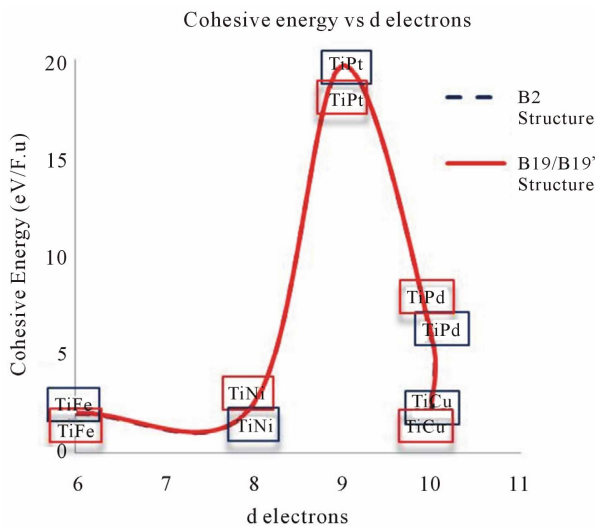


Figure 7. Variation of cohesive energy as function of “d” electrons of X in TiX (X = Fe, Ni, Pd, Pt and Cu) alloy.

of TiX alloys tend to increase systematically as we go from 3d to 4d to 5d metals [22]. From **Figure 8** we observe the heat of formation increases from TiFe to TiNi and then to TiPd. The TiPd alloy possesses highest heat of formation energy in B19 phase.

6. Equation of State

The total energy of TiX (X = Fe, Ni, Pd, Pt and Cu) alloys has been calculated for different reduced and extended volumes and fitted with the sixth order polynomial. From the first derivative of the polynomial the P-V data of TiX (X = Fe, Ni, Pd, Pt and Cu) in their stable structures are generated. Vinet *et al.* have proposed a universal equation of state which is valid for all the classes of solids under compression. The UEOS is expressed as

$$P = 3B_0 (1-x)/x^2 \exp[\eta(1-x)] \quad (3)$$

where x denotes $(V/V_0)^{1/3}$ and B_0 refers to the bulk modulus. If one defines $H(x) = x^2 P(x)/[3(1-x)]$, then the $\ln[H(x)]$ versus $1-x$ curve should be linear and obey the relation

$$\ln[H(x)] \approx \ln B_0 + \eta(1-x) \quad (4)$$

The bulk modulus of TiX alloys in B2 and (B19/B19') structures are given in **Table 3** and shown in **Figure 9**. From the bulk modulus curve, for B19 the B_0 value is found to be maximum for 5d TiPt followed by 4d TiPd and 3d TiNi. Generally, the compounds with high melting temperature T_m are expected to have high B_0 value. The melting temperatures of TiPt, TiPd and TiNi are 1830 K, 1673 K and 1583 K, respectively. Thus, a systematic trend between B_0 and T_m is observed in B19

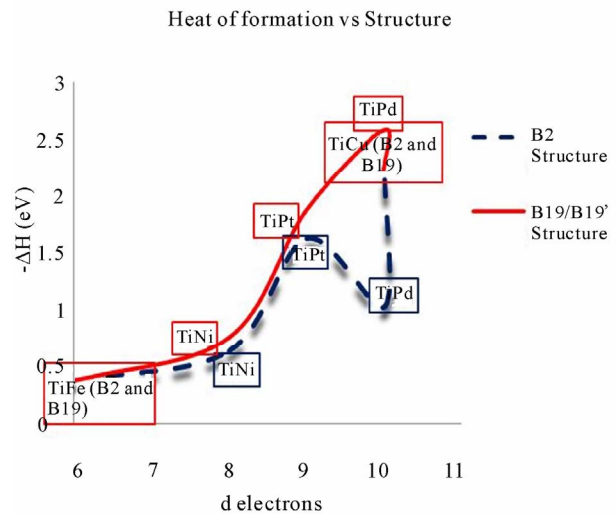


Figure 8. Variation of heat of formation as function of “d” electrons of X in TiX (X = Fe, Ni, Pd, Pt and Cu) alloys.

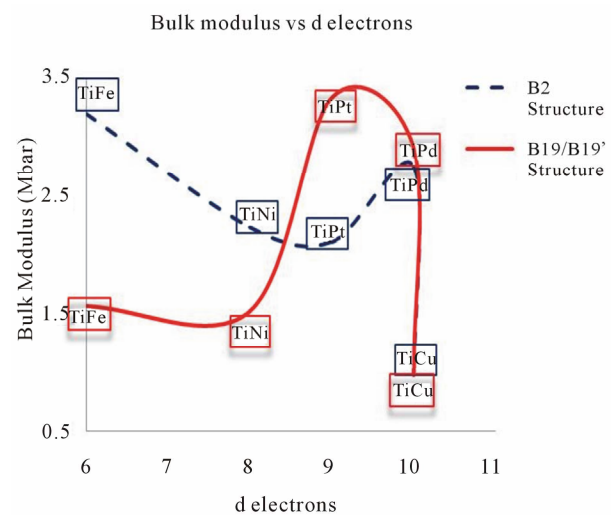


Figure 9. Variation of Bulk modulus as function of “d” electrons in TiX (X = Fe, Ni, Pd, Pt and Cu) alloy.

phase. In case of B2 phase, we infer bulk modulus values to decrease gradually as a function of d electrons except for TiPd. The B_0 value is higher for TiPd than for TiPt. The T_m is defined by both bulk modulus and the shear modulus. So, the observation of no systematic trend between B_0 and T_m in B2 phase indicates that the shear contribution varies significantly among these compounds in this phase. The bulk modulus of TiNi in B2 phase computed from our total energy study is 2.2984 Mbar which is higher than the values 1.56 Mbar reported by Y. Ye *et al.* It has been experimentally and theoretically observed that the ternary alloying of V with TiNi [23,24] will enhance the hardness of the alloy. The present work show that the hardness of TiPd is larger than that of TiNi

hence alloying of TiNi with Pd substitution will improve the hardness of the material [19,25].

7. Conclusions

We have performed first principles local density functional electronic structure calculation for the five TiX alloys (X = Fe, Ni, Pd, Pt and Cu) using the TB-LMTO method. From our theoretical total-energy studies on TiX alloys we have arrived at the following conclusions:

- The calculated lattice constants are found to be in good agreement with experimental results.
- All alloys exist in B2 structure at ground state. The electronic properties are rather similar for these alloys as they have same number of valence electrons. If we look at fine details, the properties of TiFe and TiNi are similar and that of TiPd and TiPt are closer to each other than to TiNi.
- From the DOS histogram, we observe the lower energy part of the DOS curve to be dominated by the X metal d states and the higher energy part dominated by the Ti d states. The DOS at E_F is mainly contributed by the Ti d states except for TiFe alloy wherein d states of Fe show more dominance. The DOS localization accompanied by the spatial localization of d electrons of X (X = Fe, Ni, Pd, Pt, Cu) atoms results in weakening of the d-d covalent bonds between the alloy components.
- The d-d hybridization is much pronounced for TiNi in B19' phase and p-d hybridization for TiPd and TiPt in B19 phase.
- The calculated heat of formation is higher for B19/B19' structure showing a positive indication of strong directional bonding in (B19/B19') phase.
- The bulk modulus value is found to be higher for the 5d series followed by 3d and then by 4d series of transition elements for B2 phase.

REFERENCES

- [1] J. Morgiel, "Ordering of the β Phase in TiNiCu and TiNi-CuMn Melt Spun Ribbons Studied with the ALCHEMI Technique," *Materials Chemistry and Physics*, Vol. 81, No. 2-3, 2003, pp. 230-232. [doi:10.1016/S0254-0584\(02\)00556-4](https://doi.org/10.1016/S0254-0584(02)00556-4)
- [2] S. A. Shabalovskaya, "Phase Transitions in the Intermetallic Compound TiNi with Charge-Density Wave Formation," *Physica Status Solidi (B)*, Vol. 132, No. 2, 1985, pp. 327-344. [doi:10.1002/pssb.2221320202](https://doi.org/10.1002/pssb.2221320202)
- [3] Y. Y. Ye, C. T. Chan and K. M. Ho, "Structural and Electronic Properties of the Martensitic Alloys TiNi, TiPd and TiPt," *Physical Review B*, Vol. 56, No. 7, 1997, pp. 3678-3679. [doi:10.1103/PhysRevB.56.3678](https://doi.org/10.1103/PhysRevB.56.3678)
- [4] H. L. Skriver, "The LMTO Method," Springer, Heidelberg, 1984.
- [5] O. K. Anderson and O. Jepsen, "Explicit, First-Principles Tight-Binding Theory," *Physical Review Letters*, Vol. 53, 1984, pp. 2571-2574. [doi:10.1103/PhysRevLett.53.2571](https://doi.org/10.1103/PhysRevLett.53.2571)
- [6] V. von Barth and L. Hedin, "A Local Exchange-Correlation Potential for the Spin Polarized Case," *Journal of Physics C: Solid State Physics*, Vol. 5, No. 13, 1972, pp. 1673-1642. [doi:10.1088/0022-3719/5/13/012](https://doi.org/10.1088/0022-3719/5/13/012)
- [7] O. Jepsen and O. K. Anderson, "The Electronic Structure of h.c.p Ytterbium," *Solid State Communications*, Vol. 9, No. 20, 1971, pp. 1763-1767. [doi:10.1016/0038-1098\(71\)90313-9](https://doi.org/10.1016/0038-1098(71)90313-9)
- [8] P. Blochl, "Gesamtenergien, Kräfte und Metall-Halbleiter Grenzflächen (Total Energies, Forces and Metal-Semiconductor Interfaces)," PhD Thesis, University of Stuttgart, Stuttgart, 1989.
- [9] J. M. Zhang and G. Y. Guo, "Electronic and Phase Stability of Three Series of B2 Ti-Transition-Metal Compound," *Journal of Physics: Condensed Matter*, Vol. 7, No. 30, 1995, p. 6001. [doi:10.1088/0953-8984/7/30/006](https://doi.org/10.1088/0953-8984/7/30/006)
- [10] M. Sanati, R. C. Albers and F. J. Pinski, "Electronic and Crystal Structure of NiTi Martensite," *Physical Review B*, Vol. 58, No. 20, 1998, pp. 13590-13593. [doi:10.1103/PhysRevB.58.13590](https://doi.org/10.1103/PhysRevB.58.13590)
- [11] Y. Kudoh, M. Tokonami, S. Miyazaki and Kotsuka, "Crystal Structure of the Martensite in Ti-49.2 at% Ni Alloy Analyzed by the Single Crystal X-Ray Diffraction Method," *Acta Metallurgica*, Vol. 33, No. 11, 1985, pp. 2049-2056. [doi:10.1016/0001-6160\(85\)90128-2](https://doi.org/10.1016/0001-6160(85)90128-2)
- [12] P. Ravindran and R. Asokamani, "Electronic Structure, Phase Stability, Equation of State and Pressure Dependent Superconducting Properties of Zr_3Al ," *Physical Review B*, Vol. 50, No. 2, 1994, pp. 668-673. [doi:10.1103/PhysRevB.50.668](https://doi.org/10.1103/PhysRevB.50.668)
- [13] V. L. Maruzz, J. F. Janak and K. Schwarz, "Calculated Thermal Properties of Metals," *Physical Review B*, Vol. 37, No. 2, 1988, pp. 790-799. [doi:10.1103/PhysRevB.37.790](https://doi.org/10.1103/PhysRevB.37.790)
- [14] A. Gyobu, Y. Kawamura, H. Horikawa and T. Saburi, "Martensitic Transformation and Two-Way Shape Memory Effect of Sputter-Deposited Ni-Rich Ti-Ni Alloy Films," *Materials Science and Engineering: A*, Vol. 273, 1999, pp. 749-753. [doi:10.1016/S0921-5093\(99\)00409-8](https://doi.org/10.1016/S0921-5093(99)00409-8)
- [15] G. Bihlmayer, R. Eibler and A. Nickel, "Electronic Structure of B2-NiTi and -PdTi," *Journal of Physics C: Solid State Physics*, Vol. 5, 1993, pp. 5083-5090.
- [16] H. J. Liu and Y. Ye, "Electronic Structure and Stability of Ti-Based Shape Memory Alloys by LMTO-ASA," *Solid State Communications*, Vol. 106, No. 4, 1998, pp. 197-202. [doi:10.1016/S0038-1098\(98\)00008-8](https://doi.org/10.1016/S0038-1098(98)00008-8)
- [17] P. Ravindran and R. A. Asokmani, "Ground-State Properties and Relative Stability between the $L1_2$ and DO_a Phases of Ni_3Al by Nb Substitution," *Physical Review B*, Vol. 53, No. 3, 1996, pp. 1129-1137.
- [18] S. A. Shabalovskaya and A. Narmonev, "Electronic Structure and Stability of Ti-Based B2 Shape-Memory Compounds: X-Ray and Ultraviolet Photoelectron Spectra," *Physical Review B*, Vol. 48, No. 18, 1993, pp. 13296-13311. [doi:10.1103/PhysRevB.48.13296](https://doi.org/10.1103/PhysRevB.48.13296)
- [19] G. Cacciamani, J. De keyzer, R. Ferro and U. E. Klotz,

- “Critical Evaluation of the Fe-Ni, Fe-Ti and Fe-Ni-Ti Alloy Systems,” *Intermetallics*, Vol. 14, No. 11, pp. 1312-1325.
[doi:10.1016/j.intermet.2005.11.028](https://doi.org/10.1016/j.intermet.2005.11.028)
- [20] J. Cai, D. S. Wang, S. J. Liu, S. Q. Duan and B. K. Ma, “Electronic Structure and B2 Phase Stability of Ti-based Shape-Memory Alloys,” *Physical Review B*, Vol. 60, No. 23, 1999, pp. 15691-15698.
[doi:10.1103/PhysRevB.60.15691](https://doi.org/10.1103/PhysRevB.60.15691)
- [21] P. Vajeeston, P. Ravindran, C. Ravi and R. Asokamani, “Electronic Structure, Bonding, and Ground-State Properties of AlB_2 -Type Transition-Metal Diborides,” *Physical Review B*, Vol. 63, No. 4, 2001, pp. 5115-5126.
[doi:10.1103/PhysRevB.63.045115](https://doi.org/10.1103/PhysRevB.63.045115)
- [22] G. Bozzolo, R. D. Noebe, H. O. Mosca, “Site Preference of Ternary Alloying Additions to NiTi: Fe, Pt, Pd, Au, Al, Cu, Zr and Hf,” *Journal of Alloys and Compounds*, Vol. 389, No. 1-2, 2005, pp. 80-94.
[doi:10.1016/j.jallcom.2004.07.051](https://doi.org/10.1016/j.jallcom.2004.07.051)
- [23] R. F. Decker and J. R. Mihalisin, “Coherency Strains in γ Hardened Nickel Alloys,” *Transactions of the American Society of Metals Quarterly*, Vol. 62, 1969, pp. 481-489.
- [24] J. H. Xu, T. Oquchi and A. J. Freeman, “Phase Stability and Magnetism of Ni_3Al ,” *Physical Review B*, Vol. 41, No. 8, 1990, pp. 5010-5016.
[doi:10.1103/PhysRevB.41.5010](https://doi.org/10.1103/PhysRevB.41.5010)
- [25] K. P. Mohancachandra, D. Shin and G. P. Carman, “Deposition and Characterization of Ti-Ni-Pd and Ti-Ni-Pt Shape Memory Alloy Thin Films,” *Smart Materials and Structures*, Vol. 14, No. 5, 2005, pp. 312-316.
[doi:10.1088/0964-1726/14/5/021](https://doi.org/10.1088/0964-1726/14/5/021)